Published online 1 June 2016

Nucleic Acids Research, 2016, Vol. 44, No. 15 ***7281–7291***
doi: 10.1093/nar/gkw485

The structure and duplex context of DNA interstrand crosslinks affects the activity of DNA polymerase η

Upasana Roy[1], Shivam Mukherjee[1], Anjali Sharma[2], Ekaterina G. Frank[3] and Orlando D. Schärer[1,2,*]

[1]Department of Chemistry, Stony Brook University, Stony Brook, NY 11794-3400, USA, [2]Department of Pharmacological Sciences, Stony Brook University, Stony Brook, NY 11794-3400, USA and [3]Laboratory of Genomic Integrity, National Institute of Child Health and Human Development, National Institutes of Health, Bethesda, MD 20892-3371, USA

Received February 24, 2016; Revised April 29, 2016; Accepted May 20, 2016

ABSTRACT

Several important anti-tumor agents form DNA interstrand crosslinks (ICLs), but their clinical efficiency is counteracted by multiple complex DNA repair pathways. All of these pathways require unhooking of the ICL from one strand of a DNA duplex by nucleases, followed by bypass of the unhooked ICL by translesion synthesis (TLS) polymerases. The structures of the unhooked ICLs remain unknown, yet the position of incisions and processing of the unhooked ICLs significantly influence the efficiency and fidelity of bypass by TLS polymerases. We have synthesized a panel of model unhooked nitrogen mustard ICLs to systematically investigate how the state of an unhooked ICL affects pol η activity. We find that duplex distortion induced by a crosslink plays a crucial role in translesion synthesis, and length of the duplex surrounding an unhooked ICL critically affects polymerase efficiency. We report the synthesis of a putative ICL repair intermediate that mimics the complete processing of an unhooked ICL to a single crosslinked nucleotide, and find that it provides only a minimal obstacle for DNA polymerases. Our results raise the possibility that, depending on the structure and extent of processing of an ICL, its bypass may not absolutely require TLS polymerases.

INTRODUCTION

Interstrand crosslinks (ICLs) are highly cytotoxic DNA lesions formed by a number of bifunctional alkylating agents used in cancer chemotherapy, including cisplatin, nitrogen mustards and mitomycin C. ICLs covalently link the two strands of a DNA duplex, preventing strand separation and blocking essential processes such as replication and transcription (1,2). The cytotoxic effect of blocking DNA metabolism in tumor cells with high proliferation rates is the basis of the therapeutic value of ICLs as anticancer agents. One of the limitations of using ICLs in the clinic is that the complex cellular pathways that remove ICLs from the genomes of tumor cells, lead to the occurrence of resistance to such treatment (3).

In vertebrates, the predominant pathways for ICL repair are coupled to replication and involve multiple cellular pathways including Fanconi anaemia (FA), translesion DNA synthesis (TLS), homologous recombination (HR) as well as the activity of endo- and exonucleases (4,5). Although multiple pathways for ICL repair exist, a pathway defined in replication competent *Xenopus* egg extracts using plasmids containing site-specific ICLs has provided a mechanistic framework for understanding ICL repair (6). In this system, two replication forks converge on an ICL, with one leading strand extending up to 1 nt before the ICL, and the other leading strand stalling 20–40 nt before the ICL (6,7) (Supplementary Figure S1, (ii)). Arrival of the leading strand at the ICL triggers the FA pathway and FANCD2/FANCI ubiquitylation, leading to dual incisions around the ICL on the opposing parental strand to generate an 'unhooked ICL' that still remains attached to one strand (Supplementary Figure S1, (iii) and (iv)) (8). The endonuclease ERCC1-XPF has been shown to be required for these incisions (9) and this step is believed to involve other endo- or exonucleases, possibly SNM1A or SLX1 (10–12). One of the open questions is at what distance from the ICL the incisions occur. The position of the incisions influences the subsequent step, the extension of the leading strand past the unhooked ICL by TLS polymerases (Supplementary Figure S1, (v)). Following full extension past the ICL, the newly synthesized strand is ligated to the downstream Okazaki fragments, restoring one of the daughter duplexes (Supplementary Figure S1, (vii)), therefore providing a template to repair the other sister chromatid by HR. NER is believed to remove the remnant of the unhooked ICL, completing the repair process. In the *Xenopus* system, the ICL remnant has

*To whom correspondence should be addressed. Tel: +1 631 632 7545; Email: orlando.scharer@stonybrook.edu

been observed still attached to the parent strand after completion of the replication of both strands of the plasmid, most likely as a single crosslinked nucleotide (6).

A critical step in ICL repair is the bypass of the unhooked ICL by DNA polymerases. This step may lead to the introduction of mutations at or around the ICL site as it is mediated by error-prone TLS polymerases. These enzymes have been furthermore implicated in mediating chemoresistance to crosslinking drugs (13–15). Although it is unknown where the incisions are made during the unhooking step in ICL repair and how many nucleotides surround the ICL (12) (Supplementary Figure S1, (iii) and (iv)), it is thought that unhooked ICLs can be accommodated in the enlarged active sites and bypassed by TLS polymerases (16). Evidence from genetic and functional assays suggests a key role for pol ζ and Rev1 in ICL repair (6,17–21). Additional enzymes, including pol η (22–24), pol κ (25,26) or pol υ (27,28) have also been implicated in ICL repair, suggesting that the choice of polymerase may depend on the structure of ICLs and the pathways used. *In vitro* studies have demonstrated that pol η, pol κ, pol ι and pol υ can bypass a variety of different ICLs (25,27,29–31). These studies have shown that the efficiency of bypass depends on the structure of the ICL itself, and in particular also on the length of the duplex surrounding the crosslink. While ICLs in long duplexes (∼20 base pairs) were hardly bypassed by any of the polymerases, several enzymes were able to bypass ICLs in duplexes of 2–5 base pairs.

Here, we report a more detailed structure-function relationship of pol η on a panel of nitrogen mustard-like ICLs. The most important biological role of pol η is the error-free bypass of UV-induced cyclobutane pyrimidine dimers (CPD) and mutations of the protein in humans are associated with the cancer-prone syndrome xeroderma pigmentosum variant (XP-V) (32,33). However, pol η deficiency also causes sensitivity to crosslinking agents (22–24) and pol η upregulation in tumors is associated with resistance to treatment with cisplatin and nitrogen mustards (15,34). Our studies dissect and quantify the effect of DNA distortion, flexibility of the ICL and position of incisions on translesion synthesis by pol η. We furthermore report a new strategy to synthesize the most extensively resected form of an ICL possible, a putative single nucleotide crosslinked intermediate, and find that it only represents a minimal obstacle for DNA polymerases.

MATERIALS AND METHODS

Synthesis of 2-aminoethyl 7-deazaguanosine

Full experimental procedures and analytical data for the synthesis of 2-aminoethyl-7-deazaguanosine are available in the Supplementary Information.

Oligonucleotides and primers

The following oligonucleotides were synthesized for the generation of ICLs as described (35,36) containing 7-deaza-dG aldehyde ICL precursors denoted as 'X' (see Supplementary Figure S2 for the three 7-deaza-dG crosslink precursors used):

T39 (39mer): 5′-GAAAGAAG**X**ACAGAAGAGGGT ACCATCATAGAGTCAGTG-3′ C20 (20mer): 5′-CCCT CTUCT**X**TCCUTCTTTC-3′.

The following primers for the polymerase reactions containing a 5′ FAM fluorescent label were purchased from IDT technologies:

P15: 5′-(6-FAM)CACTGACTCTATGATG-3′;

P0: 5′-(6-FAM)GACTCTATGATGGTACCCTCTTC TGT-3′

Preparation of 20 bp and 6 bp ICLs

ICLs were generated as described (29,37) (Supplementary Figure S3). The T39 and C20 oligonucleotides containing the ICL precursors were annealed, oxidized with 50 mM $NaIO_4$ in 100 mM sodium phosphate buffer (pH 5.4), and excess oxidizing agent removed by washing with 10 mM sodium phosphate buffer (pH 5.4) using Amicon Ultracel 3K columns (cat. no. UFC500396). ICLs were formed by treatment with either 5 mM hydrazine (HY) or 5 mM N,N-dimethylethylenediamine (DA) in the presence of $NaBH_3CN$. The coupling reaction was incubated overnight in the dark at room temperature, and the ICLs were purified by 12–15% denaturing PAGE. ICLs were extracted from the gel by electroelution using the Scheicher & Schuell BT1000 Biotrap system according to manufacturer's instructions in 5 mM $Na_2B_4O_7$ (pH 8.0). To generate the resected 6 bp ICLs, the purified 20 bp ICLs were digested with the USER enzyme mix (uracil DNA glycosylase and endonuclease VIII, NEB M5505), which cleaved the phosphodiester backbone at the position of the uracil residues. The 6 bp ICLs were purified by 12–15% denaturing PAGE followed by electroelution as described above.

Preparation of single nucleotide (1 nt) ICLs

A solution of an 11mer oligonucleotide (20 nmols, 100 μl) (5′-GAAAGAAG**X**AC-3′) containing the C2 ICL precursor (Supplementary Figure S2) was treated with 10 μl of 50 mM $NaIO_4$ and allowed to stand overnight in the dark at 4°C. Excess $NaIO_4$ was removed by washing with 10 mM sodium phosphate buffer (pH 5.4) using Amicon Ultracel 3K columns (cat. no. UFC500396). The ICL was formed by adding 10 μl of 0.5 M solution of 7-(2-aminoethyl)-7-deazaguanosine (**3**) and 10 μl of 0.5 M $NaCNBH_3$ and incubation overnight in the dark at room temperature. The product and starting material were separated on a 20% denaturing PAGE gel and the ICL band was excised under UV-light. The band was extracted with 0.5 M NH_4OAc using the crush and soak method. The identity of the ICL band was confirmed using MALDI-TOF mass spectrometry (m/z calculated: 3683; found 3676) (Supplementary Figure S4). To generate T39 containing the single nucleotide ICL, the purified 11-mer with the single nucleotide ICL was ligated to a 5′-phosphorylated 28-mer (5′P-AGAAGA GGGTACCATCATAGAGTCAGTG-3′). The two oligos (500 nM each) were annealed to a complementary 51-mer splint (1 μM, 5′-TTGGAACACTGACTCTATGATGGT ACCCTCTTCTGTCCTTCTTTCGTTAAC-3) in 10 mM Tris-HCl pH 8.0, 50 mM NaCl overnight at room temperature. The annealed oligonucleotides were incubated with

T4 DNA ligase (NEB M0202S) for 30 min at 37°C. Products were resolved by 15% denaturing PAGE and the 39-mer containing single nucleotide ICL was extracted from the gel by electroelution as described above.

Enzymes

Klenow (exo-) enzyme (5 U/μl equivalent to 3.6 μM) was purchased from NEB (M0212). The protein was diluted in 25 mM Tris-Cl (pH 7.4), 1 mM DTT, 0.1 mM ethylenediamine-tetraacetic acid (EDTA) and 50% glycerol to the indicated concentrations for use in polymerase assays. Human pol η (with a C terminal His tag) was prepared as described previously, yielding a preparation with a concentration of 0.3 mg/ml (∼4 μM) (38). The protein was diluted in 40 mM Tris-HCl (pH 8.0), 10 mM dithiothreitol (DTT), 0.1 mg/ml bovine serum albumin (BSA) and 30% glycerol to the indicated concentrations for use in polymerase assays.

Polymerase assays

ICL substrates (150 nM) and 6-FAM labeled primer P15 (50 nM) were annealed in 10 mM Tris-HCl pH 8.0, 50 mM NaCl, overnight at room temperature to ensure the stability of the ICLs. The ICL substrates/primers (5 nM, with respect to the primer) and 100 μM dNTPs were incubated with DNA polymerase in a reaction volume of 10 μl. For assays with Klenow (exo-), 1 nM enzyme was used in reaction buffer NEB2 (50 mM NaCl, 10 mM Tris-HCl, 10 mM $MgCl_2$, 1 mM DTT). A total of 40 nM pol η was used in a reaction buffer containing 40 mM Tris-Cl pH 8.0, 50 mM NaCl, 5 mM $MgCl_2$, 10 mM DTT and 2.5% glycerol. Reactions were incubated for 10 min at 37°C and stopped by addition of 10 μl of formamide buffer (80% formamide, 1 mM EDTA, 1 mg/ml Orange G), denatured at 95°C for 2 min and chilled on ice. The products of the reaction were resolved on a 10% 7 M Urea PAGE and FAM labeled DNA was visualized using a Typhoon 9400 scanner (GE Healthcare). Images were analyzed and quantified using ImageQuant software (Molecular Dynamics (MD)).

Single nucleotide insertion assays

ICL substrates were annealed to 6-FAM labeled P0 primer as described above. All reactions were incubated for 5 min at 37°C with 1 nM Klenow (exo-) or 20 nM pol η using the reaction buffers described above. Reactions were stopped by addition of 10 μl of formamide buffer (80% formamide, 1 mM EDTA, 1 mg/ml Orange G) and products analyzed by denaturing PAGE as described for the polymerase assays.

Analysis of single nucleotide insertion assays

Since the efficiency of primer extension is different for our various substrates (high for undamaged DNA and low for 6 bp ICLs), to compare fidelity of insertion across these substrates, a 'normalized intensity' value was used instead of 'percent primer extension'. This value was calculated for each nucleotide taking into account the efficiency of nucleotide insertion for that substrate, such that 'normalized intensity' for a single nucleotide = (band intensity of lane A/T/C/G) ÷ (band intensity of lane 'N') for each substrate. For each dNTP incorporation, the bands at position 0 and +1 were combined for the measurement of band intensity, as both the insertion and extension products involved dNTP incorporation.

RESULTS

Design of NM ICL substrates mimicking unhooked repair intermediates

Nitrogen mustards preferentially crosslink two guanines in a duplex within a –GNC– sequence via their N7 positions (Figure 1A) (39). This major groove ICL induces a bend of about 20° in the DNA duplex, as the length of the ICL is shorter than the distance between the two N7 of the guanine bases it connects (36,40–42). Using a strategy previously developed in our lab (35–37) (Supplementary Figure S3), we synthesized a substrate containing a stable site-specific NM ICL mimic (which we denote 5a for a crosslink with 5 atoms) along with variants containing 6 atom (6a) and 8 atom (8a) ICLs (Figure 1B). Our molecular modeling studies have shown that the 5a ICL, like its native nitrogen mustard (NM) equivalent, induces a bend of about 20° in the DNA duplex (36). Based on the length of the ICLs, we expect the 6a ICL to have less distortion than the 5a ICL and our preliminary NMR studies have shown that the 8a ICL is intact B-form DNA and free of distortion (Guainazzi, A., de los Santos, C., ODS, unpublished observations).

We and others have previously shown that the length of the dsDNA around an ICL dramatically influences the efficiency of bypass and that a long duplex (∼10 bp) on either side of the ICL prevents bypass by TLS polymerases (25,27,29–31). In our reactions, unmodified ssDNA (Figure 1C, (i)), ssDNA containing our ICL precursor (Figure 1C, (ii), see Supplementary Figure S2B, (i) for structure) and dsDNA with our ICL precursor on the template strand (Figure 1C, (iii)) were used as uncrosslinked controls. We generated substrates with the 5a, 6a and 8a ICLs embedded in a 20mer duplex (5a/20 bp, 6a/20 bp and 8a/20 bp, respectively, Figure 1C, (iv)). As in our previous study, we also generated a resected ICL, by partially degrading the duplex around the ICL at uracil residues incorporated into the duplex to yield an ICL with a 6 mer duplex around it (6 bp ICLs) (Figure 1C, (v)). The most completely processed form of an unhooked ICL is a 'single nucleotide ICL' (1 nt ICL), in which exonucleases resect an unhooked ICL down to a single nucleotide (Figure 1C, (vi)) (43). The strategy to generate such an ICL by incorporation and cleavage of uracil residues was unsuccessful due to the failure of uracil DNA glycosylase (UNG) to cut immediately adjacent to the ICL. Therefore, we developed a synthetic route based on our double reductive amination approach to generate the single nucleotide ICLs.

Synthesis of the single nucleotide NM ICL

The single nucleotide NM ICL (1 nt ICL) was synthesized by coupling 7-(2-aminoethyl)-deazaguanosine **3** to our aldehyde-containing ICL precursor T39. The synthesis of **3** began with the allyl **1** (35) (Figure 2), in which the

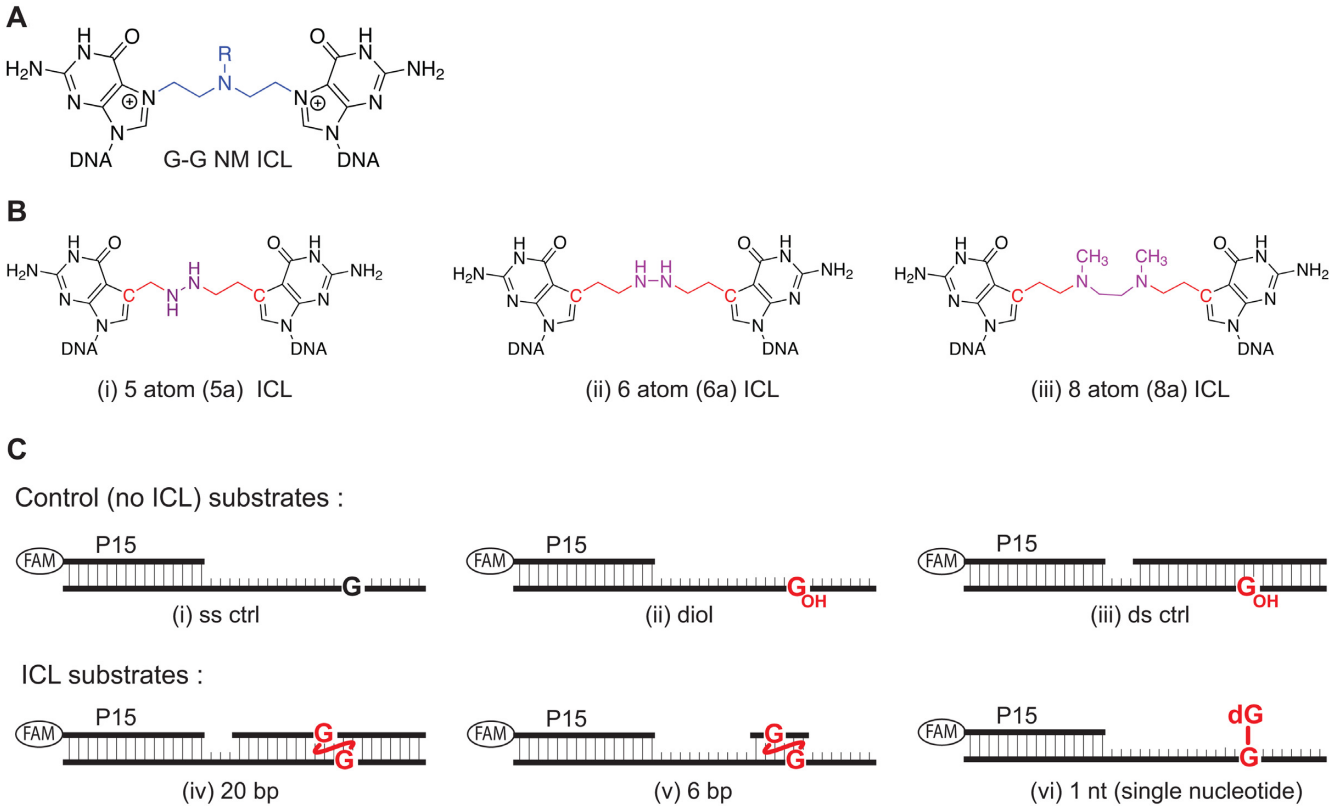

Figure 1. ICL substrates used in this study. (**A**) Structure of a nitrogen mustard (NM) ICL linking two guanine bases. (**B**) Structure of the 5 atom ((i), 5a), 6 atom ((ii), 6a) and 8 atom ((iii), 8a) NM ICL. (**C**) Substrates used for polymerase assay substrates reactions. 5′-FAM labeled primer P15 was annealed to various templates. (i) single stranded DNA undamaged control (ii) single stranded substrate with ICL precursor 'diol' (Supplementary Figure S3B, i, C2) (iii) double stranded substrate with ICL precursor 'diol', (iv) ICL substrate within a 20 bp duplex, (v) ICL substrate within a 6 bp duplex (vi) single nucleotide ICL substrate. Crosslinked or adducted bases are highlighted in red.

double bond was oxidized to the diol with osmium tetroxide, oxidized to the aldehyde with sodium periodate and trapped with O-methyl-hydroxylamide **2** to form the oxime. Zinc reduction and removal of the protecting groups yielded amine **3**, which was reacted with a 11mer single-stranded oligonucleotide containing a C2 aldehyde ICL precursor **4** under reductive amination conditions (Figure 2B). Analysis of the reaction products by denaturing PAGE revealed the formation of a slower moving band, indicating the formation of the desired product (Figure 2C). Isolation and analysis of the product by mass spectrometry revealed it to be the target single nucleotide ICL (Supplementary Figure S4). In our polymerase assays we compared the single nucleotide ICL to that of our stable C2 ICL precursor—a deazaguanine residue substituted with a dihydroxypropyl group (diol) (Supplementary Figure S3B, (i))—in the template strand to asses the effect of a single nucleotide ICL versus a smaller lesion (Figure 1C, (ii)).

Reducing duplex around ICL facilitates bypass

TLS is believed to occur in three stages: approach of the replicative or TLS polymerase up to the lesion, insertion of a dNTP across the lesion and extension past the lesion, often with different polymerases carrying out the insertion and extension steps (44–46). Keeping this in mind, we evaluated our primer extension assays in three parts (Figure 3A): 'Approach' (extension of primers up to 1 nt before the crosslinked base (−1)), 'Insertion' (insertion opposite the ICL up to 3 nt past it (0 to +3)) and 'Extension' (all products from +4 to the full length product). We chose to include 3 nucleotides in the 'insertion' category as we previously observed that some TLS polymerases have prominent stalling points at and within a few nucleotides of the insertion site (29).

In a first set of experiments, we aimed to understand how the length of duplex around an ICL—reflecting the position of incisions during unhooking—would affect translesion DNA synthesis. Using the 5a NM ICL mimic (Figure 1B, (i)) in the 20 bp, 6 bp and 1 nt substrates (Figure 1C, (iv–vi)), we first used the bacterial replicative polymerase, exonuclease deficient Klenow fragment as a benchmark. As we have found previously (29), Klenow stalled predominantly at −1 in the 20 bp ICL (Figure 3B, lane 5). In the 6 bp ICL, resection of the duplex allowed ∼30% insertion opposite the ICL, introducing a stalling at position 0 in addition to the main stalling point at −1, without any further extension to full product (Figure 3B, compare lanes 4 and 5).

As expected, there was no stalling at the G residue on the ssDNA template (Figure 3B, lane 1). With the single stranded C2 ICL precursor (diol) (Figure 1C, (ii) and Sup-

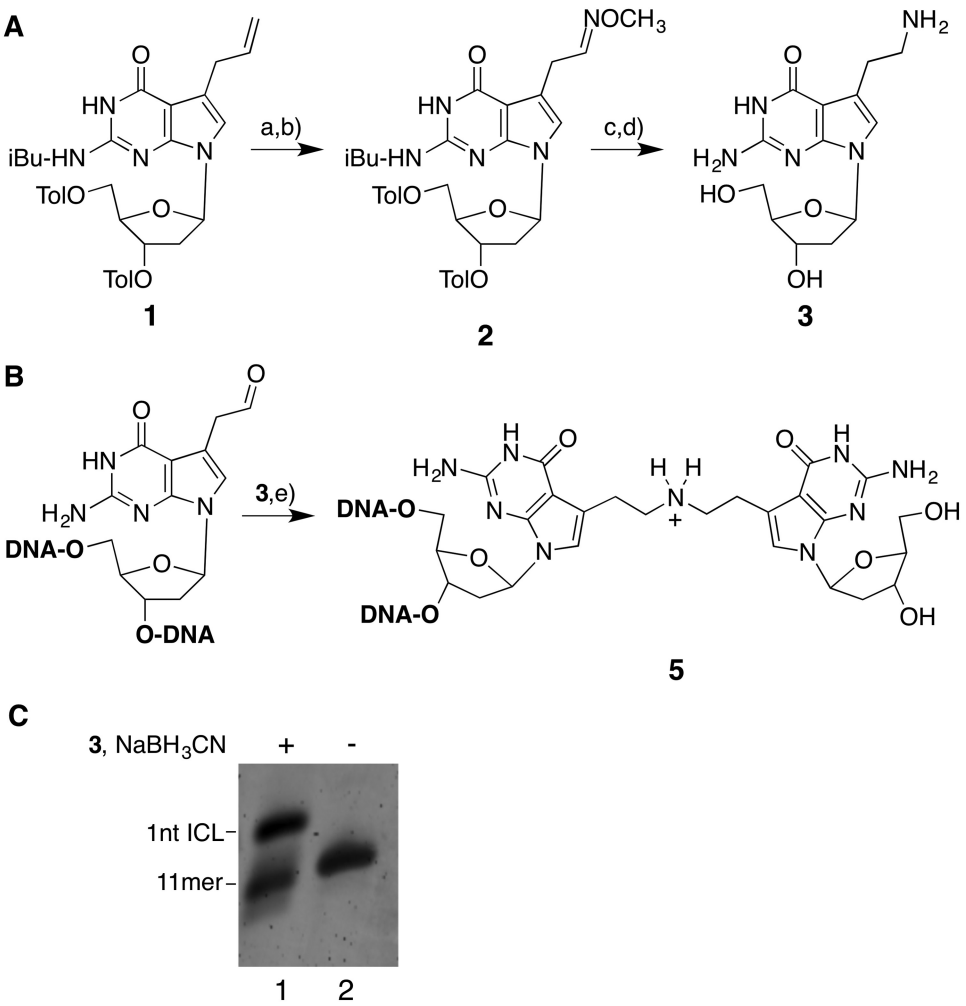

Figure 2. Synthesis of the single nucleotide ICL. (**A**) Reaction conditions: (a) OsO_4, NMM, THF, 0°C, 72%; (b) (i) $NaIO_4$, MeOH, THF; (ii) NH_2OMe, 86%; (c) Zn/HCl, MeOH, HOAc, 85%; (d) NH3, MeOH. (**B**) (e) (i) $NaIO_4$, H_2O (ii) $NaBH_3CN$. (**C**) 20% denaturing PAGE analysis of reaction of the 11mer (GAAAGAAG**4**AC) with amine **3**. DNA was visualized with SYBR gold.

plementary Figure S3B, (i)), there was a pausing at the 0 and −1 positions, while most of the primer was extended to the full length product (Figure 3B, lane 2), suggesting that a substitution at the N7 position is only a minor impediment for Klenow, consistent with the frequent modification at that position for DNA sequencing and other applications (47). Interestingly, a similar pattern was observed for the single nucleotide (1 nt) ICL (Figure 3B, lane 3), with only a pausing site at the crosslinked base, accompanied by efficient bypass of the ICL (Figure 3C). This result raises the possibility that some forms of unhooked ICLs may be bypassed by a replicative polymerase and that a TLS polymerase may not always be absolutely required for ICL repair.

We then assayed the activity of TLS polymerase pol η with the various ICLs. Pol η also stalled during approach to the ICL in the 5a/20 bp substrate, but was able to insert a nucleotide opposite the ICL and at the +1 position (Figure 3D and E). The approach and insertion by pol η was significantly facilitated in the 5a/6 bp ICL, with the +1 and +2 insertion products making up close to 70% of the products. The amount of fully extended product was however still limited. Interestingly, the 5a/1 nt ICL, similar to the single stranded undamaged DNA (ss) and C2 ICL precursor (diol) was bypassed by pol η with high efficiency, resulting primarily in extension of the primers to full length products. These findings show that the amount of duplex around an ICL greatly affected the efficiency of pol η to bypass ICLs, and that at least in the case of a fully processed 1 nt ICL, pol η could carry out both insertion and extension steps alone.

NM ICL-induced distortion facilitates approach and insertion, but inhibits extension by pol η

NM ICLs cause a slight local distortion in the surrounding duplex by introducing a bend of about 20° in the DNA helix (36), and we were interested to understand how this influenced the ability of pol η to bypass the ICL. We addressed this by using NM ICL variants with longer linkers (6a and 8a versus 5a of the NM ICL mimic) that are expected to have less or no distortion, respectively (Figure 1B). We generated the 5a, 6a and 8a ICLs embedded in 6 or 20 bp du-

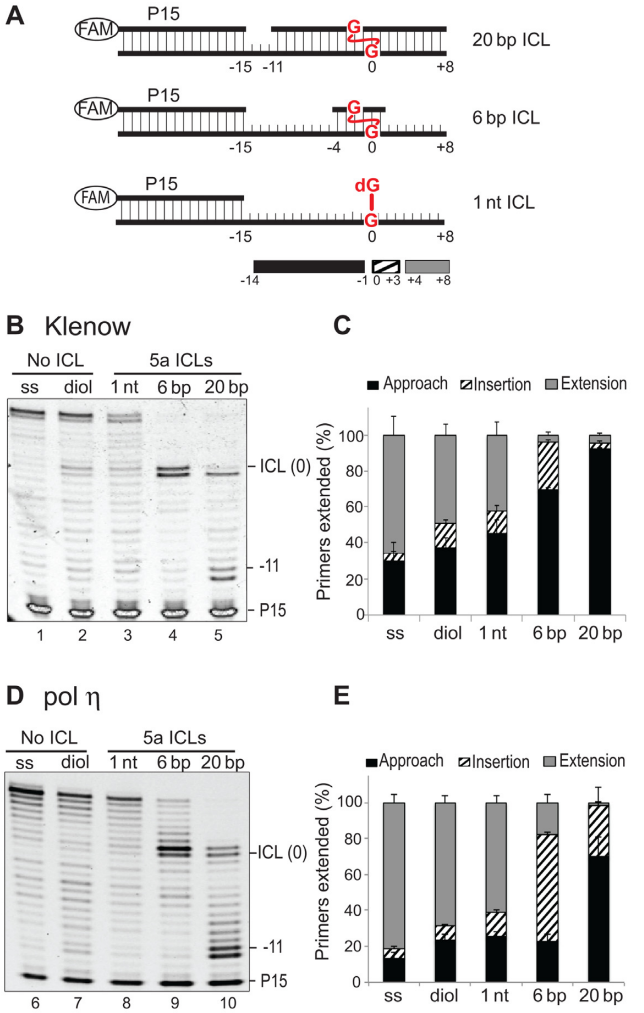

Figure 3. Shortening of duplex around the ICL facilitates bypass. (**A**) 20 bp, 6 bp and 1 nt ICL substrates used. The crosslinked base in the template strand was designated '0', and all primer extension products up to −1 were evaluated as 'approach', from 0 to +3 as 'insertion' and beyond +4 as 'extension'. (**B–E**) Translesion synthesis assay of 5a ICL templates with Klenow and pol η. Unmodified (lanes 1 and 6), diol (monoadduct, lanes 2 and 7) and 5a ICL-containing templates (lanes 3–5, 8–10) were annealed to the FAM labeled primer P15 and incubated with (**B**) 1 nM Klenow, (**D**) 40 nM pol η for 10 min at 37°C. Products were resolved by 10% denaturing PAGE. Quantification and analysis of primer extension products with (**C**) Klenow and (**E**) pol η. Each lane was divided into approach, insertion and extension segments and corresponding band intensities expressed as a percentage of the total products combined. Data represent the mean of three experiments and error bars indicate S.D.

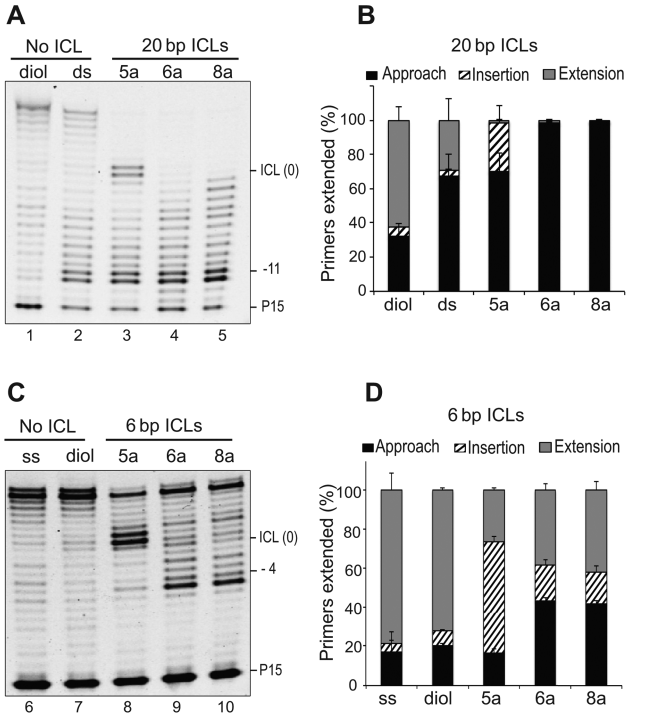

Figure 4. Duplex distortion facilitates approach and insertion by pol η at the ICL. Control and monoadduct (lanes 1–2, 6–7) and 5a, 6a and 8a ICL templates in a (**A**) 20 bp duplex (lanes 3–5) or (**C**) 6 bp duplex (lanes 8–10) were annealed to primer P15 and incubated with 40 nM pol η for 10 mins at 37°C. The products were resolved by 10% denaturing PAGE. Quantification and analysis of primer extension products with 20 bp ICLs (**B**) and 6 bp ICLs (**D**). Each lane was divided into approach, insertion and extension segments and corresponding band intensities expressed as a percentage of all the products combined. Data represent the mean of three experiments and error bars indicate S.D.

plexes and annealed them to fluorescently labeled primers for the analysis of bypass by pol η. Pol η was able to insert a nucleotide at the 0 and +1 position in the 5a/20 bp template (Figure 4A, lane 3). By contrast, the enzyme stalled at the −1 position with the 6a and 8a/20 bp ICLs with no detectable extension to full products (Figure 4A, lanes 4 and 5). Our data suggest that the distortion caused by the 5a ICL facilitates insertion by pol η. We speculate that the greater stability of the crosslinked duplexes without distortion (6a and 8a ICLs) resists strand displacement and therefore approach and insertion. Interestingly, the increased flexibility of the 8a linker compared to the 6a linker had no significant effect on the efficiency of insertion, suggesting that the relief of the distortion and not the additional flexibility is key to the outcome of the reaction (Figure 4B and D, compare 6a and 8a).

We then asked whether duplex destabilization would play an equally important role in promoting bypass when the amount of duplex surrounding the ICL is reduced to 6 base pairs. We found that also with the ICLs within a shorter duplex, distortion facilitated the approach to the ICL. In the reaction with the 5a/6 bp ICL, the main stalling points were at the +1 and +2 positions (Figure 4C, lane 8), while for both the non-distorting 6a/6 bp and 8a/6 bp ICLs, primer extension stalled at the beginning of the duplex (Figure 4C, lanes 9 and 10). Interestingly, there was no stalling point for the 6a and 8a ICLs at or around the crosslinked base, and once pol η was able to initiate the strand displacement reaction, most of the primer was extended to the full length product (Figure 4C, compare lane 8 to lane 9 and 10). Therefore, pol η is able to efficiently insert dNTPs opposite the non-distorting ICL and extend the primer to the full length product.

One reason for the lower insertion activity of pol η on non-distorting ICLs could be a relatively weak strand displacement ability of the enzyme. Duplex destabilization

could therefore facilitate approach and insertion across the ICL. This led us to ask whether the duplex destabilization would be equally important for a polymerase with a stronger strand displacement activity, such as Klenow. We found that there is also a significant difference in approach between distorting and non-distorting ICLs with Klenow (Supplementary Figure S5). While the initial strand displacement was similar for the 5a, 6a and 8a/20 bp ICLs, Klenow was able to extend the primer to the 0 and −1 position for the 5a ICL, while it stalled at the −3, −2 and −1 positions for the 6a and 8a ICLs (Supplementary Figure S5A, lanes 3–5). Very similar observations were made for the equivalent 6 bp ICLs, where Klenow stalled primarily at −1 and 0 for the 5a/6 bp ICL and at −2 and −1 for the 6a and 8a/6 bp ICLs (Supplementary Figure S5B, lanes 8–10). This suggests that duplex destabilization by a distorting crosslink is important in determining the efficiency of the approach to, and bypass of ICLs by polymerases with widely different strand displacement abilities.

Finally, we tested whether our observed effects on bypass depend only on the length of a crosslink or whether they are also influenced by its chemical composition. For this purpose, we used two ICLs with 6 atom linkers: 6a and 6a', which differ in that 6a has a hydrazine and 6a' has an amine linkage (Supplementary Figure S6 A). The reactions with the two 6 atom ICLs were very similar for the 6 bp and 20 bp ICLs with Klenow (Supplementary Figure S6 B), and the 20 bp ICL with pol η (Supplementary Figure S6C). The only minor difference observed was with the 6 bp ICL and pol η, where the ICL with the amine linkage seemed to be bypassed more efficiently, primarily as the strand displacement reaction appeared to be more efficient. However, quantification of the bypass reactions indicated that this may not be a significant difference. (Supplementary Figure S6B and C).

Pol η is more accurate on NM ICLs than on undamaged DNA

Like all TLS polymerases, pol η is a low fidelity enzyme, yet it has the ability to efficiently and accurately replicate past UV-induced CPDs thereby preventing UV-induced mutations (48,49). We therefore investigated how NM ICL structure affected the fidelity of dNTP insertion by pol η at the lesion site. We carried out single nucleotide incorporation assays with pol η by annealing primer P0 to the undamaged control, single nucleotide (5a/1 nt), and 5a, 6a and 8a/6 bp substrates using different concentrations of the individual dNTPs (Figure 5A).

As already observed in our bypass assays, the efficiency of primer extension was lower for the ICLs than for undamaged DNA (Figure 5B, lanes 'N'). To control for different efficiencies of dNTP incorporation for the various substrates, we quantified and used the ratio of incorporation of each individual nucleotide (A/T/C/G) to that of the four dNTPs (N) as our 'normalized relative intensity'.

At 1 μM dNTP concentration, pol η incorporated primarily dCTP – at least 2-fold more than the incorrect dNTPs, opposite the ICLs or the undamaged control G residue (Figure 5B and C). At the next higher dNTP concentration, 10 μM, incorporation opposite the control G became more promiscuous, with only about 1.2–1.4-fold higher incorporation of dCTP (Figure 5B and D). Interestingly, incorporation opposite the ICLs was more accurate than opposite an undamaged dG residue, with at least 4-fold lower incorporation of dATP and dGTP than dCTP. The misincorporation of purines opposite the ICLs was significantly lower even at 100 μM dNTP concentrations, (Figure 5B and E), where all four dNTPs were incorporated with similar efficiency opposite the control G and 5a/1 nt ICL. Although differences were minor, longer ICL linkages (8a and 6a versus 5a) allowed for higher fidelity of incorporation (compare Figure 5D and E). It is interesting to note that the fidelity of incorporation was significantly greater for the ICL surrounded by a 6 bp duplex compared to the 1 nt ICL. Collectively, our data suggest that pol η has a higher fidelity of dNTP incorporation opposite an NM ICL than unmodified DNA.

DISCUSSION

Multiple pathways for ICL repair have been described which share as one common feature the bypass of an unhooked ICL by DNA polymerases. This step restores one of the two strands modified by the ICL as a template for repair synthesis. To date it has not been possible to determine what the structures of unhooked ICLs look like. These structures are determined by several factors including the ICL repair pathway used and the positions of the incisions at the ICL (12). As a result, replicative and translesion synthesis polymerases are likely to encounter a variety of unhooked ICL structures. In this study, we investigated the reaction of the Y-family TLS polymerase pol η with a set of diverse model unhooked NM ICL structures that reflect different points of incision during unhooking, and ICL structures with different degrees of helix distortions and flexibilities.

The influence of helix distortion and ICL resection on polymerase activity

We and others have shown that resection of the duplex around an ICL greatly facilitates bypass across various ICLs (25,27,29–31). This is likely due to a reduced need for strand displacement synthesis during approach to the ICL and due to the increased flexibility of a shorter duplex during insertion and extension of the ICL. Our data (Figures 3 and 4) show that a duplex-distorting crosslink facilitates strand displacement, while non-distorting ICLs inhibit it. Similarly, in studies with *Xenopus* egg extracts, the approach to the ICL was more efficient for a highly distorting cisplatin ICL compared to a non-distorting nitrogen mustard-like ICL (6). These observations suggest that the need for resection of the duplex around an ICL may be especially important for the repair of non-distorting crosslinks. Mechanistically, this resection could be performed by hSNM1A-an exonuclease implicated in ICL repair with demonstrated ability to digest duplex DNA around an ICL (10,50). Cells lacking hSNM1A were more sensitive to exposure to the crosslinking agent MMC and SJG-136, which form non-distorting ICLs, than to nitrogen mustards, which form more distorting ICLs (10). This suggests that the exonuclease activity of hSNM1A is more important for repair of non-distorting crosslinks. Our data provide a possible explanation for why exonucleolytic processing of the duplex

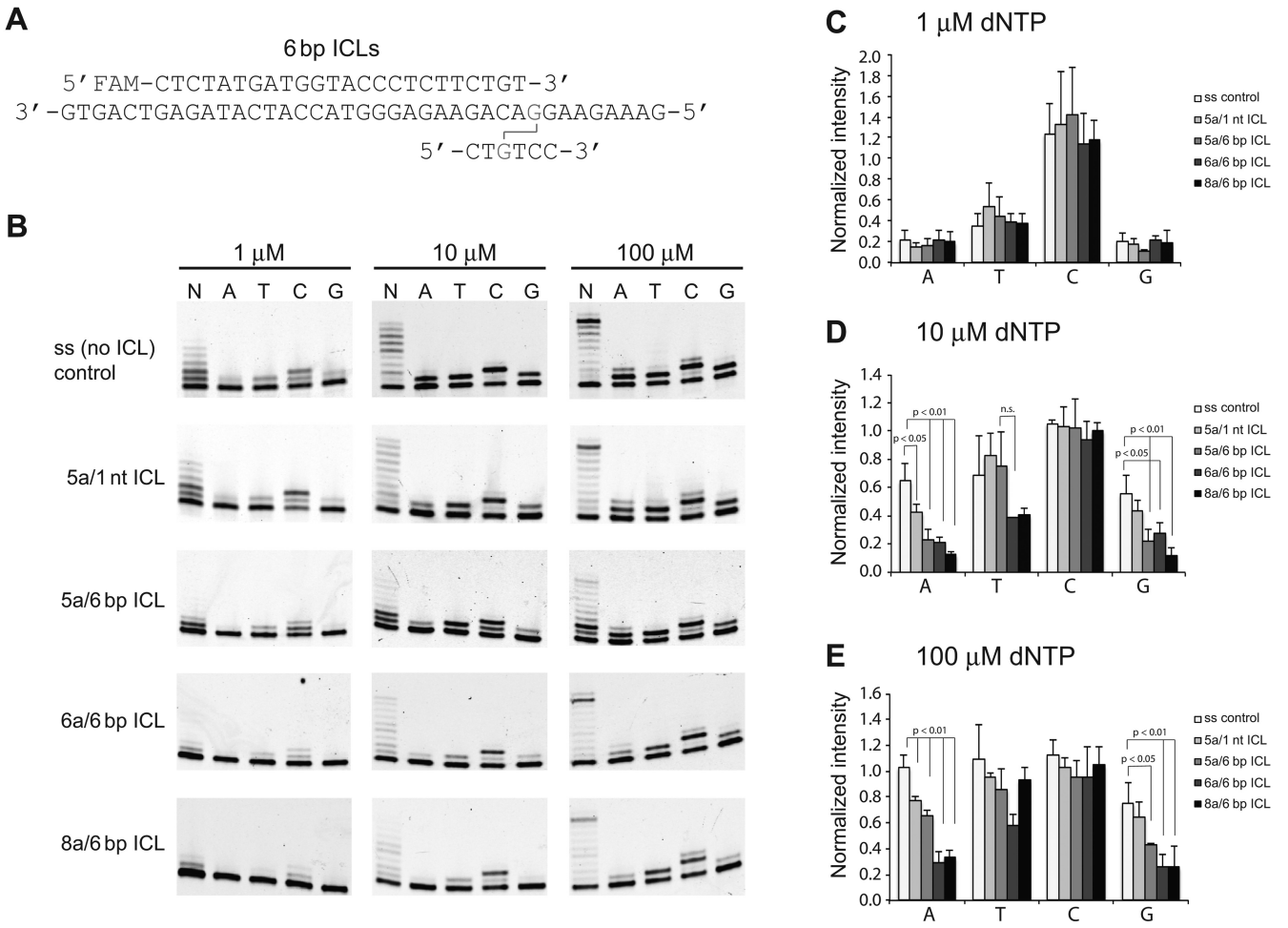

Figure 5. pol η is more accurate across NM ICLs than undamaged DNA. (**A**) Sequence of ICL substrate for single base insertion assays. (**B**) Templates were annealed to FAM labeled P0 primer and incubated with 20 nM pol η at 37°C for 5 min with 1, 10 or 100 μM of individual dNTPs (A/T/C/G) or all four dNTPs combined (N). The products were resolved by 10% denaturing PAGE and band intensities quantified using ImageQuant. Quantification and analysis of single nucleotide incorporation with (**C**) 1 μM dNTPs (**D**) 10 μM dNTPs and (**E**) 100 μM dNTPs. The ratio of band intensity for each individual nucleotide (lane A/T/C/G) to that of the four dNTPs combined (lane N) was calculated and expressed as the 'normalized intensity'. Data are represented as the mean of three experiments and error bars indicate S.D. *P*-values were calculated by a one-way ANOVA with the Bonferroni correction for multiple comparisons.

around an ICL would be more important for such non-distorting ICLs. Taken together this suggests duplex distortion and/or destabilization by an ICL is an important determinant of how lesions are processed, approached and bypassed in ICL repair.

Bypass of a single nucleotide NM ICL

One of the open questions in ICL repair is where incisions occur in the unhooking step and how much duplex surrounds the ICL when it is encountered by DNA polymerases. Two observations suggest that resection to a single nucleotide ICL might occur: (i) In experiments with *Xenopus* egg extracts an ICL remnant has been observed upon completion of replication and repair of an ICL-containing plasmid with a single nucleotide crosslinked to the template strand (6). (ii) The hSNM1A exonuclease, implicated in ICL repair, has been shown to be capable of digesting a duplex across an ICL down to a singe nucleotide, providing a mechanism for how such intermediates may be generated (10,50). Similarly, FAN1 has been shown to be able to digest a DNA duplex across an ICL (51,52).

We devised a strategy to synthesize single nucleotide NM ICLs to study how such an intermediate interacts with polymerases. Intriguingly, this ICL did not provide an obstacle for pol η, alleviating the characteristic stalling points of pol η especially after dNTP insertion opposite the ICL (Figure 3D). This observation suggests that pol η can completely bypass such structures on its own, and that ICL repair may not always require other TLS polymerases such as REV1/pol ζ to carry out the extension step. It will be interesting to see if this would also apply to ICLs such as those formed by cisplatin or psoralen that would more severely constrain the structures of single nucleotide ICL intermediates.

Interestingly, we found that the bacterial replicative polymerase Klenow was also able to bypass the single nucleotide NM ICL (5a/1 nt ICL) (Figure 3B). An earlier study using

artificial model ICLs which link two strands through the exocyclic amine groups of dC or through the N3 positions of dT residues found that single nucleotide ICLs capable of forming Watson–Crick base pairs could be bypassed by Klenow (43). Together these observations raise the intriguing possibility that some ICLs, in the most processed form, may not require the activity of a TLS polymerase to be repaired. Given that the approach to the ICL is most likely carried out by replicative polymerases (21,53), it will be interesting to see whether the mammalian replicative polymerases δ and ϵ similarly have the ability to bypass our single nucleotide NM ICL and whether it will be possible to discover a pathway of ICL repair that does not require TLS polymerases.

What could the role of pol η in ICL repair be?

Given the variety of ICL structures formed, the possible redundancy among various TLS polymerases, and the limited mechanistic resolution of current assays available for the study of ICL repair, it has been challenging to identify the polymerase(s) carrying out the insertion and extension steps on the unhooked ICLs. Based on genetic and biochemical considerations, a prime candidate for insertion across crosslinked guanines, the base most frequently modified by crosslinking agents, is the dCMP transferase REV1 (54,55). However, experiments in *Xenopus* demonstrated that REV1 and pol ζ were only required for the extension step and not the insertion across the cisplatin ICL (21) and that they were dispensable altogether for the repair of non-distorting 8 atom NM-like ICL (6). Of the alternative candidate polymerases that may instead act on these ICLs, we focused on pol η in this study. Genetic and biochemical experiments have implicated pol η in the bypass of a variety of ICLs (24,29,45,49). Structural features of pol η show this enzyme may be particularly well suited to accommodate ICLs (49,56–58). Pol η is the Y-family polymerase with the largest active site, and detailed structural studies of the enzyme bypassing CPDs have shown that it operates as a molecular splint holding on to the damaged DNA until the primer is extended 3 nucleotides past the lesion (49). Remarkably, we found that pol η extends a primer efficiently up to 2 nucleotides past an ICL in the 5a ICL, consistent with the idea that rigid binding to the primer template would allow extension by a few nucleotides past the site of insertion opposite the lesion. We think that this feature also allows for insertion and complete bypass of the more flexible 6 and 8 atom ICLs. Our results are furthermore similar to those observed with CPDs (48), in that the bypass of NM ICLs by pol η is more accurate than that of non-damaged DNA (Figure 5). These observations warrant more detailed studies of the role of pol η in the repair of different ICLs.

CONCLUSION

Using and expanding a synthetic approach in our laboratory, we generated a number of structurally diverse NM-like ICLs that differ in their degree of distortion induced in the duplex (by varying the length of the crosslink) and the amount of duplex surrounding the ICLs. Our studies indicate that more distorting (shorter) ICLs facilitate strand displacement and approach to the ICL, while less distorting (longer) ICLs are extended more efficiently after insertion. Importantly, we showed that unhooked ICL intermediates that have been processed down to a single nucleotide only pose a minimal obstacle for DNA polymerases, suggesting that the polymerase reaction past ICLs may be more facile than commonly assumed and may not always require the activity of a TLS polymerase.

SUPPLEMENTARY DATA

Supplementary Data are available at NAR Online.

ACKNOWLEDGEMENTS

The authors are grateful to Robert Rieger for help with the HR-MS and MALDI-TOF spectral analyses supported by grant NIH/NCRR 1 S10 RR023680-1, to Todor Angelov for early studies on the synthesis of 7-(2-aminoethyl)-deazaguanosine **3**, and to Roger Woodgate (NIH) for helpful discussions and comments on the manuscript.

FUNDING

NCI [R01 CA165911 to O.D.S]; NICHD Intramural Research Program (to E.G.F). Funding for open access charge: NCI [R01 CA165911].

Conflict of interest statement. None declared.

REFERENCES

1. Schärer,O.D. (2005) DNA interstrand crosslinks: natural and drug-induced DNA adducts that induce unique cellular responses. *Chembiochem*, **6**, 27–32.
2. Noll,D.M., Mason,T.M. and Miller,P.S. (2006) Formation and repair of interstrand cross-links in DNA. *Chem. Rev.*, **106**, 277–301.
3. Deans,A.J. and West,S.C. (2011) DNA interstrand crosslink repair and cancer. *Nat. Rev. Cancer*, **11**, 467–480.
4. Clauson,C., Schärer,O.D. and Niedernhofer,L. (2013) Advances in understanding the complex mechanisms of DNA interstrand cross-link repair. *Cold Spring Harbor Perspect. Biol.*, **5**, a012732.
5. Kottemann,M.C. and Smogorzewska,A. (2013) Fanconi anaemia and the repair of Watson and Crick DNA crosslinks. *Nature*, **493**, 356–363.
6. Räschle,M., Knipscheer,P., Enoiu,M., Angelov,T., Sun,J., Griffith,J.D., Ellenberger,T.E., Schärer,O.D. and Walter,J.C. (2008) Mechanism of replication-coupled DNA interstrand crosslink repair. *Cell*, **134**, 969–980.
7. Zhang,J., Dewar,J.M., Budzowska,M., Motnenko,A., Cohn,M.A. and Walter,J.C. (2015) DNA interstrand cross-link repair requires replication-fork convergence. *Nat. Struct. Mol. Biol.*, **22**, 242–247.
8. Knipscheer,P., Räschle,M., Smogorzewska,A., Enoiu,M., Ho,T.V., Schärer,O.D., Elledge,S.J. and Walter,J.C. (2009) The Fanconi anemia pathway promotes replication-dependent DNA interstrand cross-link repair. *Science*, **326**, 1698–1701.
9. Klein Douwel,D., Boonen,R.A., Long,D.T., Szypowska,A.A., Raschle,M., Walter,J.C. and Knipscheer,P. (2014) XPF-ERCC1 acts in Unhooking DNA interstrand crosslinks in cooperation with FANCD2 and FANCP/SLX4. *Mol. Cell*, **54**, 460–471.
10. Wang,A.T., Sengerová,B., Cattell,E., Inagawa,T., Hartley,J.M., Kiakos,K., Burgess-Brown,N.A., Swift,L.P., Enzlin,J.H., Schofield,C.J. *et al.* (2011) Human SNM1A and XPF–ERCC1 collaborate to initiate DNA interstrand cross-link repair. *Genes Dev.*, **25**, 1859–1870.
11. Castor,D., Nair,N., Declais,A.C., Lachaud,C., Toth,R., Macartney,T.J., Lilley,D.M., Arthur,J.S. and Rouse,J. (2013) Cooperative control of holliday junction resolution and DNA repair by the SLX1 and MUS81-EME1 nucleases. *Mol. Cell*, **52**, 221–233.

12. Zhang,J. and Walter,J.C. (2014) Mechanism and regulation of incisions during DNA interstrand cross-link repair. *DNA Repair*, **19**, 135–142.
13. Xie,K., Doles,J., Hemann,M.T. and Walker,G.C. (2010) Error-prone translesion synthesis mediates acquired chemoresistance. *Proc. Natl. Acad. Sci. U.S.A.*, **107**, 20792–20797.
14. Doles,J., Oliver,T.G., Cameron,E.R., Hsu,G., Jacks,T., Walker,G.C. and Hemann,M.T. (2010) Suppression of Rev3, the catalytic subunit of Pol{zeta}, sensitizes drug-resistant lung tumors to chemotherapy. *Proc. Natl. Acad. Sci. U.S.A.*, **107**, 20786–20791.
15. Srivastava,A.K., Han,C., Zhao,R., Cui,T., Dai,Y., Mao,C., Zhao,W., Zhang,X., Yu,J. and Wang,Q.E. (2015) Enhanced expression of DNA polymerase eta contributes to cisplatin resistance of ovarian cancer stem cells. *Proc. Natl. Acad. Sci. U.S.A.*, **112**, 4411–4416.
16. Ho,T.V. and Schärer,O.D. (2010) Translesion DNA synthesis polymerases in DNA interstrand crosslink repair. *Env. Mol. Mutagen.*, **51**, 552–566.
17. Sonoda,E., Okada,T., Zhao,G.Y., Tateishi,S., Araki,K., Yamaizumi,M., Yagi,T., Verkaik,N.S., van Gent,D.C., Takata,M. *et al.* (2003) Multiple roles of Rev3, the catalytic subunit of pol[zeta] in maintaining genome stability in vertebrates. *EMBO J.*, **22**, 3188–3197.
18. Nojima,K., Hochegger,H., Saberi,A., Fukushima,T., Kikuchi,K., Yoshimura,M., Orelli,B.J., Bishop,D.K., Hirano,S., Ohzeki,M. *et al.* (2005) Multiple repair pathways mediate tolerance to chemotherapeutic cross-linking agents in vertebrate cells. *Cancer Res.*, **65**, 11704–11711.
19. Shen,X., Jun,S., O'Neal,L.E., Sonoda,E., Bemark,M., Sale,J.E. and Li,L. (2006) REV3 and REV1 play major roles in recombination-independent repair of DNA interstrand cross-links mediated by monoubiquitinated proliferating cell nuclear antigen (PCNA). *J. Biol. Chem.*, **281**, 13869–13872.
20. Sarkar,S., Davies,A.A., Ulrich,H.D. and McHugh,P.J. (2006) DNA interstrand crosslink repair during G1 involves nucleotide excision repair and DNA polymerase zeta. *EMBO J.*, **25**, 1285–1294.
21. Budzowska,M., Graham,T.G., Sobeck,A., Waga,S. and Walter,J.C. (2015) Regulation of the Rev1-pol zeta complex during bypass of a DNA interstrand cross-link. *EMBO J.*, **34**, 1971–1985.
22. Misra,R.R. and Vos,J.M. (1993) Defective replication of psoralen adducts detected at the gene-specific level in xeroderma pigmentosum variant cells. *Mol. Cell. Biol.*, **13**, 1002–1012.
23. Albertella,M.R., Green,C.M., Lehmann,A.R. and O'Connor,M.J. (2005) A role for polymerase η in the cellular tolerance to cisplatin-induced damage. *Cancer Res.*, **65**, 9799–9806.
24. Chen,Y.-W., Cleaver,J.E., Hanaoka,F., Chang,C.-F. and Chou,K.-M. (2006) A novel role of DNA polymerase η in modulating cellular sensitivity to chemotherapeutic agents. *Mol. Cancer Res.*, **4**, 257–265.
25. Minko,I.G., Harbut,M.B., Kozekov,I.D., Kozekova,A., Jakobs,P.M., Olson,S.B., Moses,R.E., Harris,T.M., Rizzo,C.J. and Lloyd,R.S. (2008) Role for DNA polymerase κ in the processing of N^2-N^2-guanine interstrand cross-links. *J. Biol. Chem.*, **283**, 17075–17082.
26. Williams,H.L., Gottesman,M.E. and Gautier,J. (2012) Replication-independent repair of DNA interstrand crosslinks. *Mol. Cell*, **47**, 140–147.
27. Zietlow,L., Smith,L.A., Bessho,M. and Bessho,T. (2009) Evidence for the involvement of human DNA polymerase N in the repair of DNA interstrand cross-links. *Biochemistry*, **48**, 11817–11824.
28. Moldovan,G.-L., Madhavan,M.V., Mirchandani,K.D., McCaffrey,R.M., Vinciguerra,P. and D'Andrea,A.D. (2010) DNA polymerase POLN participates in cross-link repair and homologous recombination. *Mol. Cell. Biol.*, **30**, 1088–1096.
29. Ho,T.V., Guainazzi,A., Derkunt,S.B., Enoiu,M. and Schärer,O.D. (2011) Structure-dependent bypass of DNA interstrand crosslinks by translesion synthesis polymerases. *Nucleic Acids Res.*, **39**, 7455–7464.
30. Yamanaka,K., Minko,I.G., Takata,K.-I., Kolbanovskiy,A., Kozekov,I.D., Wood,R.D., Rizzo,C.J. and Lloyd,R.S. (2010) Novel enzymatic function of DNA polymerase ν in translesion DNA synthesis past major groove DNA−peptide and DNA−DNA cross-links. *Chem. Res. Tox.*, **23**, 689–695.
31. Klug,A.R., Harbut,M.B., Lloyd,R.S. and Minko,I.G. (2012) Replication bypass of N^2-deoxyguanosine interstrand cross-links by human DNA polymerases η and ι. *Chem. Res. Toxicol.*, **25**, 755–762.
32. Masutani,C., Kusumoto,R., Yamada,A., Dohmae,N., Yokoi,M., Yuasa,M., Araki,M., Iwai,S., Takio,K. and Hanaoka,F. (1999) The XPV (xeroderma pigmentosum variant) gene encodes human DNA polymerase eta. *Nature*, **399**, 700–704.
33. Johnson,R.E., Prakash,S. and Prakash,L. (1999) Efficient bypass of a thymine-thymine dimer by yeast DNA polymerase, Pol eta. *Science*, **283**, 1001–1004.
34. Tomicic,M.T., Aasland,D., Naumann,S.C., Meise,R., Barckhausen,C., Kaina,B. and Christmann,M. (2014) Translesion polymerase eta is upregulated by cancer therapeutics and confers anticancer drug resistance. *Cancer Res.*, **74**, 5585–5596.
35. Angelov,T., Guainazzi,A. and Schärer,O.D. (2009) Generation of DNA interstrand cross-links by post-synthetic reductive amination. *Org. Lett.*, **11**, 661–664.
36. Guainazzi,A., Campbell,A.J., Angelov,T., Simmerling,C. and Schärer,O.D. (2010) Synthesis and molecular modeling of a nitrogen mustard DNA interstrand crosslink. *Chemistry*, **16**, 12100–12103.
37. Mukherjee,S., Guainazzi,A. and Schärer,O.D. (2014) Synthesis of structurally diverse major groove DNA interstrand crosslinks using three different aldehyde precursors. *Nucleic Acids Res.*, **42**, 7429–7435.
38. Frank,E.G. and Woodgate,R. (2007) Increased catalytic activity and altered fidelity of human DNA polymerase iota in the presence of manganese. *J. Biol. Chem.*, **282**, 24689–24696.
39. Millard,J.T., Raucher,S. and Hopkins,P.B. (1990) Mechlorethamine cross-links deoxyguanosine residues at 5′-GNC sequences in duplex DNA fragments. *J. Am. Chem. Soc.*, **112**, 2459–2460.
40. Rink,S.M. and Hopkins,P.B. (1995) A mechlorethamine-induced DNA interstrand cross-link bends duplex DNA. *Biochemistry*, **34**, 1439–1445.
41. Dong,Q., Barsky,D., Colvin,M.E., Melius,C.F., Ludeman,S.M., Moravek,J.F., Colvin,O.M., Bigner,D.D., Modrich,P. and Friedman,H.S. (1995) A structural basis for a phosphoramide mustard-induced DNA interstrand cross-link at 5′-d(GAC). *Proc. Natl. Acad. Sci. U.S.A.*, **92**, 12170–12174.
42. Fan,Y.H. and Gold,B. (1999) Sequence-specificity for DNA interstrand cross-linking by alpha,omega-alkanediol dimethylsulfonate esters: Evidence for DNA distortion by the initial monofunctional lesion. *J. Am. Chem. Soc.*, **121**, 11942–11946.
43. Smeaton,M.B., Hlavin,E.M., Noronha,A.M., Murphy,S.P., Wilds,C.J. and Miller,P.S. (2009) Effect of cross-link structure on DNA interstrand cross-link repair synthesis. *Chem. Res. Toxicol.*, **22**, 1285–1297.
44. Prakash,S., Johnson,R.E. and Prakash,L. (2005) Eukaryotic translesion synthesis DNA polymerases: specificity of structure and function. *Ann. Rev. Biochem.*, **74**, 317–353.
45. Shachar,S., Ziv,O., Avkin,S., Adar,S., Wittschieben,J., Reissner,T., Chaney,S., Friedberg,E.C., Wang,Z., Carell,T. *et al.* (2009) Two-polymerase mechanisms dictate error-free and error-prone translesion DNA synthesis in mammals. *EMBO J.*, **28**, 383–393.
46. Lehmann,A.R., Niimi,A., Ogi,T., Brown,S., Sabbioneda,S., Wing,J.F., Kannouche,P.L. and Green,C.M. (2007) Translesion synthesis: Y-family polymerases and the polymerase switch. *DNA Repair*, **6**, 891–899.
47. Prober,J.M., Trainor,G.L., Dam,R.J., Hobbs,F.W., Robertson,C.W., Zagursky,R.J., Cocuzza,A.J., Jensen,M.A. and Baumeister,K. (1987) A system for rapid DNA sequencing with fluorescent chain-terminating dideoxynucleotides. *Science*, **238**, 336–341.
48. McCulloch,S.D., Kokoska,R.J., Masutani,C., Iwai,S., Hanaoka,F. and Kunkel,T.A. (2004) Preferential cis-syn thymine dimer bypass by DNA polymerase eta occurs with biased fidelity. *Nature*, **428**, 97–100.
49. Biertumpfel,C., Zhao,Y., Kondo,Y., Ramon-Maiques,S., Gregory,M., Lee,J.Y., Masutani,C., Lehmann,A.R., Hanaoka,F. and Yang,W. (2010) Structure and mechanism of human DNA polymerase eta. *Nature*, **465**, 1044–1048.
50. Allerston,C.K., Lee,S.Y., Newman,J.A., Schofield,C.J., McHugh,P.J. and Gileadi,O. (2015) The structures of the SNM1A and SNM1B/Apollo nuclease domains reveal a potential basis for their distinct DNA processing activities. *Nucleic Acids Res.*, **43**, 11047–11060.
51. Wang,R., Persky,N.S., Yoo,B., Ouerfelli,O., Smogorzewska,A., Elledge,S.J. and Pavletich,N.P. (2014) DNA repair. Mechanism of DNA interstrand cross-link processing by repair nuclease FAN1. *Science*, **346**, 1127–1130.

52. Pizzolato,J., Mukherjee,S., Schärer,O.D. and Jiricny,J. (2015) FANCD2-associated nuclease 1, but not exonuclease 1 or flap endonuclease 1, is able to unhook DNA interstrand cross-links in vitro. *J. Biol. Chem.*, **290**, 22602–22611.
53. Long,D.T., Räschle,M., Joukov,V. and Walter,J.C. (2011) Mechanism of RAD51-dependent DNA interstrand cross-link repair. *Science*, **333**, 84–87.
54. Nelson,J.R., Lawrence,C.W. and Hinkle,D.C. (1996) Deoxycytidyl transferase activity of yeast REV1 protein. *Nature*, **382**, 729–731.
55. Haracska,L., Prakash,S. and Prakash,L. (2002) Yeast Rev1 protein is a G template-specific DNA polymerase. *J. Biol. Chem.*, **277**, 15546–15551.
56. Reissner,T., Schneider,S., Schorr,S. and Carell,T. (2010) Crystal structure of a cisplatin-(1,3-GTG) cross-link within DNA polymerase eta. *Angew. Chem. Int. Ed. Engl.*, **49**, 3077–3080.
57. Zhao,Y., Biertumpfel,C., Gregory,M.T., Hua,Y.J., Hanaoka,F. and Yang,W. (2012) Structural basis of human DNA polymerase eta-mediated chemoresistance to cisplatin. *Proc. Natl. Acad. Sci. U.S.A.*, **109**, 7269–7274.
58. Silverstein,T.D., Johnson,R.E., Jain,R., Prakash,L., Prakash,S. and Aggarwal,A.K. (2010) Structural basis for the suppression of skin cancers by DNA polymerase eta. *Nature*, **465**, 1039–1043.